
Sparse Weight Activation Training

Md Aamir Raihan, Tor M. Aamodt

Department of Electrical And Computer Engineering
University of British Columbia
Vancouver, BC
{araihan, aamodt}@ece.ubc.ca

Abstract

Neural network training is computationally and memory intensive. Sparse training can reduce the burden on emerging hardware platforms designed to accelerate sparse computations, but it can also affect network convergence. In this work, we propose a novel CNN training algorithm called Sparse Weight Activation Training (SWAT). SWAT is more computation and memory-efficient than conventional training. SWAT modifies back-propagation based on the empirical insight that convergence during training tends to be robust to the elimination of (i) small magnitude weights during the forward pass and (ii) both small magnitude weights and activations during the backward pass. We evaluate SWAT on recent CNN architectures such as ResNet, VGG, DenseNet and WideResNet using CIFAR-10, CIFAR-100 and ImageNet datasets. For ResNet-50 on ImageNet SWAT reduces total floating-point operations (FLOPs) during training by 80% resulting in a $3.3\times$ training speedup when run on a simulated sparse learning accelerator representative of emerging platforms while incurring only 1.63% reduction in validation accuracy. Moreover, SWAT reduces memory footprint during the backward pass by 23% to 50% for activations and 50% to 90% for weights. Code is available at <https://github.com/AamirRaihan/SWAT>.

1 Introduction

Convolutional Neural Networks (CNNs) are effective at many complex computer vision tasks including object recognition [30, 60], object detection [59, 53] and image restoration [14, 68]. However, training CNNs requires significant computation and memory resources. Software and hardware approaches have been proposed for addressing this challenge. On the hardware side, graphics processor units (GPUs) are now typically used for training [30] and recent GPUs from NVIDIA include specialized Tensor Core hardware specifically to accelerate deep learning [49, 47, 48]. Specialized programmable hardware is being deployed in datacenters by companies such as Google and Microsoft [28, 9]. Techniques for reducing computation and memory consumption on existing hardware include those reducing the number of training iterations such as batch normalization [27] and enhanced optimization strategies [29, 15] and those reducing computations per iteration. Examples of the latter, which may be effective with appropriate hardware support, include techniques such as quantization [70, 8, 65, 62], use of fixed-point instead of floating-point [66, 10], sparsification [63] and dimensionality reduction [37]. This paper introduces *Sparse Weight Activation Training* (SWAT), which significantly extends the sparsification approach.

Training involves repeated application of forward and backward passes. Prior research on introducing sparsity during training has focused on sparsifying the backward pass. While model compression [21, 43, 39, 38, 35, 24, 40, 64, 44] introduces sparsification into the forward pass, it typically does so by introducing additional training phases which increase overall training time. Amdahl's Law [3] implies overall speedup is limited by the fraction of original execution time spent on computations that are

not sped up by system changes. To reduce training time significantly by reducing computations per training iteration it is necessary to address both forward and backward passes. SWAT introduces sparsification into both forward and backward passes and is suitable for emerging hardware platforms containing support for sparse matrix operations. Such hardware is now available. For example recently announced Ampere GPU architecture [49] includes support for exploiting sparsity. In addition, there is a growing body of research on hardware accelerators for sparse networks [50, 11, 69, 2] and we demonstrate, via hardware simulation, that SWAT can potentially train $5.9\times$ faster when such accelerators become available.

While SWAT employs sparsity it does so with the objective of *reducing training time not performing model compression*. The contributions of this paper are:

- An empirical sensitivity analysis of approaches to inducing sparsity in network training;
- SWAT, a training algorithm that introduces sparsity in weights and activations resulting in reduced execution time in both forward and backward passes of training;
- An empirical evaluation showing SWAT is effective on complex models and datasets.

2 Related work

Below we summarize the works most closely related to SWAT.

Network pruning: LeCun et al. [34] proposed removing network parameters using second-order information of the loss function to improve generalization and reduce training and inference time. More recently, pruning has been explored primarily as a way to improve the efficiency and storage requirements of inference but at the expense of increasing training time, contrary to the objective of this paper. Specifically, Han et al. [21] showed how to substantially reduce network parameters while improving validation accuracy by pruning weights based upon their magnitude combined with a subsequent retraining phase that fine-tunes the remaining weights. Regularization techniques can be employed to learn a pruned network [43, 39, 20]. Various approaches to structured pruning [64, 44, 35, 38, 24, 40], ensure entire channels or filters are removed to reduce inference execution time on the vector hardware found in GPUs.

Reducing per-iteration training overhead: MeProp [58, 63] reduces computations during training by back propagating only the highest magnitude gradient component and setting other component to zero. As shown in Section 3.2, on complex networks and models training is very sensitive to the fraction of gradient components set to zero. Liu et al. [37] proposed reducing computation during training and inference by constructing a dynamic sparse graph (DSG) using random projection. DSG incurs accuracy loss of 3% on ImageNet at a sparsity of 50%. Goli and Aamodt [19] propose to reduce backward pass computations by performing convolutions only on gradient components that change substantially from the prior iteration. They reduced the overall computation in the backward pass by up to 90% with minimum loss in accuracy. Their approach of backward pass sparsification is orthogonal to SWAT.

Sparse Learning: Sparse learning attempts to learn a sparse representation during training, generally as a way to achieve model compression and reduce computation during inference. Since sparse learning introduces sparsity during training it can potentially reduce training time but pruning weights by itself does not reduce weight gradient computation (Equation 3). Many sparse learning algorithms start with a random sparse network, then repeat a cycle of training, pruning and regrowth. Sparse Evolutionary Training (SET) [42] prunes the most negative and smallest positive weights then randomly selects latent (i.e., missing) weights for regrowth. Dynamic Sparse Reparameterization (DSR) [45] uses a global adaptive threshold for pruning and randomly regrows latent weights in a layer proportionally to the number of active (non-zero) weights in that same layer. Sparse Network From Scratch (SNFS) [12] further improves performance using magnitude-based pruning and momentum for determining the regrowth across layers. Rigging the Lottery Ticket (RigL) [17] uses an instantaneous gradient as its regrowth criteria. Dynamic Sparse Training (DST) [36] defines a trainable mask to determine which weights to prune. Recently Kusupati et al. [33] proposes a novel state-of-the-art method of finding per layer learnable threshold which reduces the FLOPs during inference by employing a non-uniform sparsity budget across layers.

Table 1: Comparison of SWAT with related works

| Algorithms | Sparsity Across Layer | Sparse Forward Pass | Sparse Backward Pass | | Unstructured Sparse Network | Structured Sparse Network |
|-----------------|-----------------------|---------------------|----------------------|-----------------|-----------------------------|---------------------------|
| | | | Input Gradient | Weight Gradient | | |
| Network Pruning | Fixed/Variable | Yes/Gradual | Yes/Gradual | No | Depend on algorithm | |
| meProp [58] | Fixed | No | Yes | Yes | No | - |
| DSG [37] | Fixed | Yes | Yes | Yes | Yes | - |
| SET [42] | Fixed | Yes | Yes | No | Yes | - |
| DSR [45] | Variable | Yes | Yes | No | Yes | - |
| SNFS [12] | Variable | Yes | Yes | No | Yes | - |
| RigL [17] | Fixed | Yes | Yes | No | Yes | - |
| SWAT | Fixed/Variable | Yes | Yes | Yes | Yes | Yes |

In contrast, SWAT employs a unified training phase where the algorithm continuously explores sparse topologies during training by employing simple magnitude based thresholds to determine which weight and activations components to operate upon. In addition, the sparsifying function used in SWAT can be adapted to induce structured sparse topologies and varying sparsity across layers. Table 1 summarizes the differences between SWAT and recent related work on increasing sparsity. The column ‘‘Sparsity Across Layer’’ indicates whether the layer sparsity is constant during training. The columns labeled ‘‘Input Gradient’’ and ‘‘Weight Gradient’’ represent whether the input gradient or weight gradient computation is sparse during training.

3 Sparse weight activation training

We begin with preliminaries, describe a sensitivity study motivating SWAT then describe SWAT and several enhancements.

3.1 Preliminaries

We consider a CNN trained using mini-batch stochastic gradient descent, where the l^{th} layer maps input activations a_{l-1} to outputs a_l using function f_l :

$$a_l = f_l(a_{l-1}, w_l) \quad (1)$$

where w_l are layer l ’s weights. During back-propagation the l^{th} layer receives the gradient of the loss with respect to its output activation (∇_{a_l}). This is used to compute the gradient of the loss with respect to its input activation ($\nabla_{a_{l-1}}$) and weight (∇_{w_l}) using function G_l and H_l respectively. Thus, the backward pass for the l^{th} layer can be defined as:

$$\nabla_{a_{l-1}} = G_l(\nabla_{a_l}, w_l), \quad (2)$$

$$\nabla_{w_l} = H_l(\nabla_{a_l}, a_{l-1}) \quad (3)$$

We induce sparsity on a tensor by retaining the values for the K highest magnitude elements and setting the remaining elements to zero. Building on the notion of a ‘‘Top-k’’ query in databases [55] and similar to Sun et al. [58] we call this process Top- K sparsification.

3.2 Sensitivity Analysis

We begin by studying the sensitivity of network convergence by applying Top- K sparsification to weights (w_l), activations (a_{l-1}) and/or back-propagated error gradients (∇_{a_l}) during training. For these experiments, which help motivate SWAT, we evaluate DenseNet-121, VGG-16 and ResNet-18 on the CIFAR-100 dataset. We run each experiment three times and report the mean value.

Figure 1 plots the impact on validation accuracy of applying varying degrees of Top- K sparsification to weights or activations during computations in the forward pass (Equation 1). In this experiment, when applying top- K sparsification in the forward pass weights or activations are not permanently

removed. Rather, low magnitude weights or activations are removed temporarily during the forward pass and restored before the backward pass. Thus, in this experiment the backward pass uses unmodified weights and activations without applying any sparsification and all weights are updated by the resulting dense weight gradient. The data in Figure 1 suggests convergence is more robust to Top- K sparsification of weights versus activations during the forward pass. The data shows that inducing high activation sparsity hurts accuracy after a certain point, confirming similar observations by Georgiadis [18] and Kurtz et al. [32].

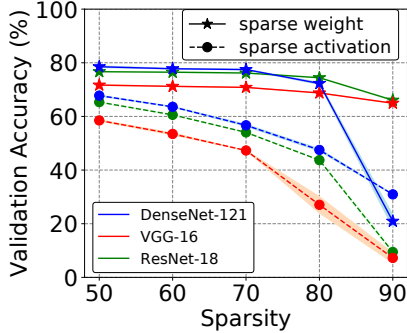


Figure 1: Forward Pass Sensitivity Analysis.

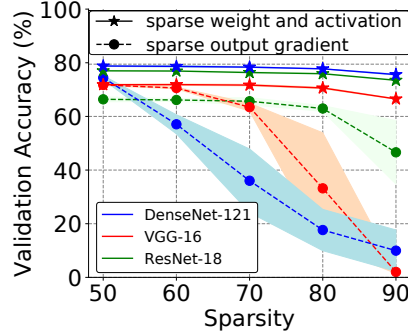


Figure 2: Backward Pass Sensitivity Analysis.

Figure 2 plots the impact on validation accuracy of applying varying degrees of Top- K sparsification to both weights and activations (labeled “sparse weight and activation”) or to only output gradients (labeled “sparse output gradient”) during computations in the backward pass (Equations 2 and 3). “Weights and activations” or “back-propagated output error gradients” are sparsified before performing the convolutions to generate weight and input gradients. The generated gradients are dense since a convolution between a sparse and dense inputs will in general produce a dense output. The resulting dense weight gradients are used in the parameter update stage. We note that this process differs, for example, from recent approaches to sparsifying inference (e.g., [33, 71, 17]) which employ dense back-propagated output gradients during convolution to generate weight gradients that are masked during the parameter update stage. The “sparse weight and activation” curve shows that convergence is relatively insensitive to applying Top- K sparsification. In contrast, the “sparse output gradient” curve shows that convergence is sensitive to applying Top- K sparsification to back-propagated error gradients (∇_{a_l}). The latter observation indicates that meProp, which drops back-propagated error-gradients, will suffer convergence issues on larger networks.

3.3 The SWAT Algorithm

The analysis above suggests two strategies: In the forward pass use sparse weights (but *not* activations) and in the backward pass use sparse weights and activations (but *not* gradients).

Sparse weight activation training (SWAT) embodies these two strategies as follows (for pseudo-code see supplementary material): During each training pass (forward and backward iteration on a mini-batch) a sparse weight topology is induced during the forward pass using the Top- K function. This partitions weights into active (i.e., Top- K) and non-active sets for the current iteration. The forward pass uses the active weights. In the backward pass, the full gradients and active weights are used in Equation 2 and the full gradients and highly activated neurons (Top- K sparsified activations) are used in Equation 3. The later generate dense weight gradients that are used to update *both* active and non-active weights. The updates to non-active weights mean the topology can change from iteration to iteration. This enables SWAT to perform dynamic topology exploration: Backpropagation with sparse weights and activations approximates backpropagation on a network with sparse connectivity and sparsely activated neurons. The dense gradients generated during back-propagation minimize loss for the current sparse connectivity. However, the updated weights resulting from the dense gradients will potentially lead to a new sparse network since non-active weights are also updated. This process captures fine-grained temporal importance of connectivity during training. Section 4.5 shows quantitatively, the importance of unmasked gradient updates and dynamic exploration of connectivity.

3.3.1 Top-K Channel Selection

Top- K sparsification induces fine-grained sparsity. SWAT can instead induce structured sparsity on weights by pruning channels. Similarly to [5, 38, 41, 35], the saliency criteria for selecting channels is L_1 norm. Figure 3 illustrates using channel L_1 norm to select 50% of channel (Top-50%). The squares on the right side contain the channel L_1 norm and lower L_1 norm channels are set as non-active (lightly shaded). The importance of channel’s is consider independently, i.e., different filters can select different active channels.

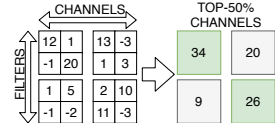


Figure 3: Top-K Channel Selection.

3.3.2 Sparsity Distribution

The objective of SWAT is to reduce training time while maintaining accuracy. So far we have assumed the per layer sparsity of weights and activations is equal to the target sparsity. Prior work [17, 12] has demonstrated that a non-uniform distribution of active weights and activation sparsity can improve accuracy for a given sparsity. We explore three strategies to distributing sparsity. All three of the following variants employ magnitude comparisons to select which tensor elements to set to zero to induce sparsity. We say an element of a tensor is unmasked if it is not forced to zero before being used in a computation. For all three techniques below the fraction of unmasked elements in a given layer is identical for weights and activations.

Uniform (SWAT-U): Similar to others (e.g., Evci et al. [17]) we found that keeping first layer dense improves validation accuracy. For SWAT-U we keep the first layer dense and apply the same sparsity threshold uniformly across all other layers.

Erdos-Renyi-Kernel (SWAT-ERK): For SWAT-ERK active weights and unmasked activations are distributed across layers by taking into account layer dimensions and setting a per layer threshold for magnitude based pruning. Following Evci et al. [17] higher sparsity is allocated to layers containing more parameters.

Momentum (SWAT-M): For SWAT-M active weights and unmasked activations are distributed across layers such that less non-zero elements are retained in layers with smaller average momentum for active weights. This approach is inspired by Dettmers and Zettlemoyer [12].

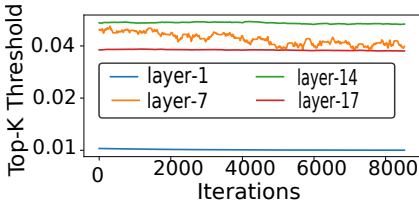


Figure 4: Top- K weight threshold versus training iteration

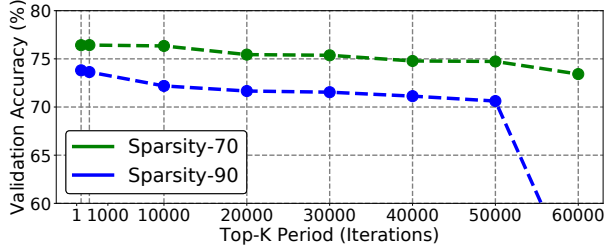


Figure 5: Impact of Top- K sampling period.

3.3.3 Efficient Top-K Threshold Calculation

The variants of SWAT described above induce sparsity by examining the magnitude of tensor elements and this incurs some overhead. Naively, the Top- K operation could be performed on a 1-dimensional array of size N in $O(N \log N)$ using sorting. The overhead can be reduced to $O(N)$ using a threshold operation where elements with magnitude greater than a threshold are retained and others are treated as zeros. The K -th largest element can be found in $O(N)$ average time complexity using Quickselect [25] or in $\theta(N)$ time using either BFPRT [4] or Introselect [46] and efficient parallel implementations of Top- K have been proposed for GPUs [55].

Figure 4 plots the threshold value required to achieve 90% weight sparsity versus training iteration for SWAT-U and unstructured pruning four representative layers of ResNet-18 while training using

CIFAR-100. This data suggests that for a given layer the magnitude of the K -th largest element is almost constant during training. Thus, we explored whether we can set a per layer threshold for weights and activations on the first iteration and only update it periodically.

Figure 5 plots the final Top-1 validation accuracy after training converges versus Top- K sampling period for SWAT-U and unstructured pruning applied to ResNet-18 trained using CIFAR 100. Here 391 iterations (x-axis) corresponds to a single epoch. The data indicates that for sampling intervals up to 1000 iterations validation accuracy is not degraded significantly.

4 Experiments

Below we present results for validation accuracy, theoretical reduction in floating-point operations (FLOPs) during training and estimates of training speedup on a simulated sparse accelerator. While **not** our primary objective we also report theoretical FLOPs reduction for inference.

4.1 Methodology

We measure validation accuracy of SWAT by implementing custom convolution and linear layers in PyTorch 1.1.0 [51]. Inside each custom PyTorch layer we perform sparsification before performing the layer forward or backward pass computation. To obtain accuracy measurements in a reasonable time these custom layers invoke NVIDIA’s cuDNN library using Pytorch’s C++ interface.

We estimate *potential* for training time reduction using an analytical model to measure total floating-point operations and an architecture simulator modeling a sparse DNN training accelerator based upon an extension of the Bit-Tactical inference accelerator [11].

We employ standard training schedules for training ResNet [22], VGG [56] with batch-normalization [27], DenseNet [26] and Wide Residual Network [67] on CIFAR10 and CIFAR100 [31]. We use SGD with momentum as an optimization algorithm with an initial learning rate of 0.1, momentum of 0.9, and weight decay λ of 0.0005. For training runs with ImageNet we employ the augmentation technique proposed by Krizhevsky et al. [30]: 224×224 random crops from the input images or their horizontal flip are used for training. Networks are trained with label smoothing [61] of 0.1 for 90 epochs with a batch size of 256 samples on a system with eight NVIDIA 2080Ti GPUs. The learning rate schedule starts with a linear warm-up reaching its maximum of 0.1 at epoch 5 and is reduced by $(1/10)$ at epochs 30^{th} , 60^{th} and 80^{th} . The optimization method is SGD with Nesterov momentum of 0.9 and weight decay λ of 0.0001. Results for ImageNet use a Top- K threshold recomputed every 1000 iterations while those for CIFAR-10 recompute the Top- K threshold every iteration. Due to time and resource constraints below we report SWAT-ERK and SWAT-M results only for CIFAR-10 and unstructured sparsity.

The supplementary material includes detailed hyperparameters, results for CIFAR-100, ablation study of the accuracy impact of performing Top- K on different subsets of weight and activation tensors.

4.2 Unstructured SWAT

CIFAR-10: Table 2 compares SWAT-U, SWAT-ERK and SWAT-M with unstructured sparsity versus published results for DST [36] and SNFS [12] for VGG-16-D, WRN-16-8, and DenseNet-121 on CIFAR-10. Under the heading “Training Sparsity” we plot the average sparsity for weights (W) and activations (Act). For SWAT-ERK and SWAT-M per layer sparsity for weights and activations are equal for a given layer but their averages for the entire network differ because these are computed by weighting by the number of weights or activations per layer. Comparing SWAT against SNFS and DST for VGG-16 and WRN-16-8 the data shows that SWAT-M has better accuracy versus SNFS and DST on both networks. While SWAT-M reduces training FLOPs by 33% and 22% versus SNFS and DST, respectively, SWAT-M requires more training FLOPs versus DST on VGG-16. SWAT-U has better accuracy versus SNFS and DST on WRN-16-8 and SWAT-U obtains $2.53\times$ and $1.96\times$ harmonic mean reduction in remaining training FLOPs versus SNFS and DST, respectively. It is important to note that the reduction in FLOPs for SWAT-ERK is competitive with SWAT-U. In general, uniform will require fewer training and inference computations versus ERK when the input resolution is high since ERK generally applies lower sparsity at the initial layer resulting in significant initial overhead. However, in Table 2, for all these networks the initial layer will have less computation

Table 2: Unstructured SWAT on the CIFAR-10 dataset. **W:** Weight, **Act:** Activation, **BA:** Baseline Accuracy, **AC:** Accuracy Change, **MC:** Model Compression, **DS:** Default Sparsity.

| Network | Methods | Training Sparsity | | Top-1 | | Training | | Inference | |
|--------------|-----------|-------------------|---------|------------------------------------|----------------------|------------------------|----------------------|-----------------|------------------------|
| | | W (%) | Act (%) | Acc. \pm SD (σ) (%) | BA / AC | FLOPs \downarrow (%) | Act \downarrow (%) | MC (\times) | FLOPs \downarrow (%) |
| VGG-16 | SNFS [12] | 95.0 | DS | 93.31 | 93.41 / -0.10 | 57.0 | DS | 20.0 | 62.9 |
| | DST [36] | 96.2 | DS | 93.02 | 93.75 / -0.73 | 75.7 | DS | 26.3 | 83.2 |
| | SWAT-U | 90.0 | 90.0 | 91.95 \pm 0.06 | 93.30 / -1.35 | 89.7 | 36.2 | 10.0 | 89.5 |
| | SWAT-ERK | 95.0 | 82.0 | 92.50 \pm 0.07 | 93.30 / -0.80 | 89.5 | 33.0 | 20.0 | 89.5 |
| | SWAT-M | 95.0 | 65.0 | 93.41 \pm 0.05 | 93.30 / +0.11 | 64.0 | 25.0 | 20.0 | 58.4 |
| WRN-16-8 | SNFS [12] | 95.0 | DS | 94.38 | 95.43 / -1.05 | 81.8 | DS | 20.0 | 88.0 |
| | DST [36] | 95.4 | DS | 94.73 | 95.18 / -0.45 | 83.3 | DS | 21.7 | 91.4 |
| | SWAT-U | 90.0 | 90.0 | 95.13 \pm 0.11 | 95.10 / +0.03 | 90.0 | 49.0 | 10.0 | 90.0 |
| | SWAT-ERK | 95.0 | 84.0 | 95.00 \pm 0.12 | 95.10 / -0.10 | 91.4 | 45.8 | 20.0 | 91.7 |
| | SWAT-M | 95.0 | 78.0 | 94.97 \pm 0.04 | 95.10 / -0.13 | 86.3 | 42.5 | 20.0 | 85.9 |
| DenseNet-121 | SWAT-U | 90.0 | 90.0 | 94.48 \pm 0.06 | 94.46 / +0.02 | 89.8 | 44.0 | 10.0 | 89.8 |
| | SWAT-ERK | 90.0 | 88.0 | 94.14 \pm 0.11 | 94.46 / -0.32 | 89.7 | 43.0 | 10.0 | 89.6 |
| | SWAT-M | 90.0 | 86.0 | 94.29 \pm 0.11 | 94.46 / -0.17 | 84.2 | 42.0 | 10.0 | 83.6 |

Table 3: Unstructured SWAT on the ImageNet dataset. **W:** Weight, **Act:** Activation, **BA:** Baseline Accuracy, **AC:** Accuracy Change, **MC:** Model Compression, **DS:** Default Sparsity.

| Network | Methods | Training Sparsity | | Top-1 | | Training | | Inference | |
|-----------|-------------|-------------------|-----------------------------------|-----------------------------------|--------------------|------------------------|----------------------|-----------------|------------------------|
| | | W (%) | Act (%) | Acc. \pm SD (σ) (%) | BA / AC | FLOPs \downarrow (%) | Act \downarrow (%) | MC (\times) | FLOPs \downarrow (%) |
| ResNet-50 | SET [42] | 80.0 | DS | 73.4 \pm 0.32 | 76.8 / -3.4 | 58.1 | DS | 3.4 | 73.0 |
| | | 90.0 | DS | 71.3 \pm 0.24 | 76.8 / -5.5 | 63.8 | DS | 5.0 | 82.1 |
| | DSR [45] | 80.0 | DS | 74.1 \pm 0.17 | 76.8 / -2.7 | 51.6 | DS | 3.4 | 59.4 |
| | | 90.0 | DS | 71.9 \pm 0.07 | 76.8 / -4.9 | 58.9 | DS | 5.0 | 70.7 |
| | SNFS [12] | 80.0 | DS | 74.9 \pm 0.07 | 77.0 / -2.1 | 45.8 | DS | 5.0 | 43.3 |
| | | 90.0 | DS | 72.9 \pm 0.07 | 77.0 / -4.1 | 57.6 | DS | 10.0 | 59.7 |
| | RigL [17] | 80.0 | DS | 74.6 \pm 0.06 | 76.8 / -2.2 | 67.2 | DS | 5.0 | 77.7 |
| | | 90.0 | DS | 72.0 \pm 0.05 | 76.8 / -4.8 | 74.1 | DS | 10.0 | 87.4 |
| | DST [36] | 80.4 | DS | 74.0 \pm 0.41 | 76.8 / -2.8 | 67.1 | DS | 5.0 | 84.9 |
| | | 90.1 | DS | 72.8 \pm 0.27 | 76.8 / -4.0 | 75.8 | DS | 10.0 | 91.3 |
| | SWAT-U | 80.0 | 80.0 | 75.2 \pm 0.06 | 76.8 / -1.6 | 76.1 | 39.2 | 5.0 | 77.7 |
| | | 90.0 | 90.0 | 72.1 \pm 0.03 | 76.8 / -4.7 | 85.6 | 44.0 | 10.0 | 87.4 |
| | SWAT-ERK | 80.0 | 52.0 | 76.0 \pm 0.16 | 76.8 / -0.8 | 60.0 | 25.5 | 5.0 | 58.9 |
| | | 90.0 | 64.0 | 73.8 \pm 0.23 | 76.8 / -3.0 | 79.0 | 31.4 | 10.0 | 77.8 |
| SWAT-M | 80.0 | 49.0 | 74.6 \pm 0.11 | 76.8 / -2.2 | 45.9 | 23.7 | 5.0 | 45.0 | |
| | 90.0 | 57.0 | 74.0 \pm 0.18 | 76.8 / -2.8 | 65.4 | 27.2 | 10.0 | 64.8 | |
| WRN-50-2 | SWAT-U | 80.0 | 80.0 | 76.4 \pm 0.10 | 78.5 / -2.1 | 78.6 | 39.1 | 5.0 | 79.2 |
| | SWAT-U | 90.0 | 90.0 | 74.7 \pm 0.27 | 78.5 / -3.8 | 88.4 | 43.9 | 10.0 | 89.0 |

due to the small input resolution of the CIFAR-10 dataset, and computationally expensive layers are allotted higher sparsity in SWAT-ERK.

The data under “Act \downarrow ” report the fraction of activation elements masked to zero, which can be exploited by hardware compression proposed by NVIDIA [54] to reduce transfer time between GPU and CPU.

ImageNet: Table 3 compares SWAT-U with unstructured sparsity against six recently proposed sparse learning algorithms at target weight sparsities of 80% and 90% on ImageNet. Data for all sparse learning algorithms except RigL were obtained by running their code using the hyperparameters in Section 4.1. Results for RigL are quoted from Evci et al. [17]. SET and DSR do not sparsify downsampling layers leading to increased parameter count. At 80% sparsity, SWAT-U attains the highest validation accuracy while reducing training FLOPs. DST trains ResNet-50 on ImageNet dataset with less computation (“Training FLOPs”) than RigL even though DST is a dense to sparse training algorithm while RigL is a sparse to sparse training algorithm. This occurs for two reasons: (1) DST quickly reaches a relatively sparse topology after a few initial epochs; in our experiment, DST discards more

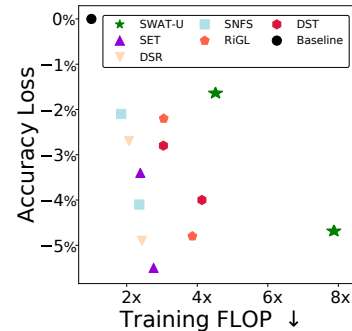


Figure 6: Accuracy decrease versus reduction in training FLOPs

Table 4: Structured SWAT on the CIFAR-10 dataset. **W:** Weight, **Act:** Activation, **CP:** Channel Pruned, **BA:** Baseline Accuracy, **AC:** Accuracy Change, **MC:** Model Compression.

| Network | Methods | Training Sparsity | | Top-1 | | Training | | Inference | |
|--------------|---------|--------------------|-----------|-----------------------------------|---------------|---------------------------|-------------------------|--------------------|---------------------------|
| | | W (%) / Act (%) | CP (%) | Acc. \pm SD (σ) (%) | BA / AC | FLOPs \downarrow (%) | Act \downarrow (%) | MC (\times) | FLOPs \downarrow (%) |
| ResNet-18 | SWAT-U | 50.0/50.0 | 50.0 | 94.73 \pm 0.06 | 94.59 / +0.14 | 49.8 | 26.0 | 2.0 | 49.8 |
| | | 60.0/60.0 | 60.0 | 94.68 \pm 0.03 | 94.59 / +0.09 | 59.8 | 31.2 | 2.5 | 59.8 |
| | | 70.0/70.0 | 70.0 | 94.65 \pm 0.19 | 94.59 / +0.06 | 69.8 | 36.4 | 3.3 | 69.8 |
| DenseNet-121 | SWAT-U | 50.0/50.0 | 50.0 | 95.04 \pm 0.26 | 94.51 / +0.53 | 49.9 | 25.0 | 2.0 | 49.9 |
| | | 60.0/60.0 | 60.0 | 94.82 \pm 0.11 | 94.51 / +0.31 | 59.9 | 30.0 | 2.5 | 59.9 |
| | | 70.0/70.0 | 70.0 | 94.81 \pm 0.20 | 94.51 / +0.30 | 69.9 | 35.0 | 3.3 | 69.9 |

Table 5: Structured SWAT on the ImageNet dataset. **W:** Weight, **Act:** Activation, **CP:** Channel Pruned, **BA:** Baseline Accuracy, **AC:** Accuracy Change, **MC:** Model Compression.

| Network | Methods | Training | | Pruning | | Top-1 | | Inference | |
|-----------|-------------------|--------------------|---------------------------|-------------------------|-----------|----------------------|------------------|---------------|---------------------------|
| | | W (%) / Act (%) | FLOPs \downarrow (%) | Act \downarrow (%) | CP (%) | Fine-Tune (epoch) | Acc (%) | BA / AC | FLOPs \downarrow (%) |
| ResNet-50 | DCP [72] | - | Offline Pruning | - | - | 60 | 74.95 | 76.01 / -1.06 | 55.0 |
| | CCP [52] | - | Offline Pruning | - | 35 | 100 | 75.50 | 76.15 / -0.65 | 48.8 |
| | AOFP [13] | - | Offline Pruning | - | - | Yes (-) | 75.11 | 75.34 / -0.23 | 56.73 |
| | Soft-Pruning [23] | - | - | - | 30 | No | 74.61 | 76.15 / -1.54 | 41.8 |
| | SWAT-U | 50.0/50.0 | 47.6 | 24.5 | 50 | No | 76.51 \pm 0.30 | 76.80 / -0.29 | 48.6 |
| | (Structured) | 60.0/60.0 | 57.1 | 29.5 | 60 | No | 76.35 \pm 0.06 | 76.80 / -0.45 | 58.3 |
| | (Structured) | 70.0/70.0 | 66.6 | 34.3 | 70 | No | 75.67 \pm 0.06 | 76.80 / -1.13 | 68.0 |
| WRN-50-2 | SWAT-U | 50.0/50.0 | 49.1 | 24.5 | 50 | No | 78.08 \pm 0.20 | 78.50 / -0.42 | 49.5 |
| | (Structured) | 60.0/60.0 | 58.9 | 29.4 | 60 | No | 77.55 \pm 0.07 | 78.50 / -0.95 | 59.4 |
| | (Structured) | 70.0/70.0 | 68.7 | 34.2 | 70 | No | 77.19 \pm 0.11 | 78.50 / -1.31 | 69.3 |

than 70% of network parameter within 5 epochs; (2) The sparsity distribution across layers is the crucial factor deciding reduction in FLOPs since allocating higher sparsity to the computationally expensive layer alleviates the initial overhead during entire training. Therefore, the overall benefit of DST is dependent on network architecture, sparsity distribution, and the parameter discard rate. Figure 6 plots the reduction in validation accuracy versus the reduction in training FLOPs relative to baseline dense training at both 80% and 90% sparsity using the same data as Table 3. This figure shows SWAT-U provides the best tradeoff between validation and reduction in training FLOPs.

4.3 Structured SWAT

CIFAR10: Table 4 provides results for SWAT-U with channel pruning on the CIFAR-10 dataset. At 70% sparsity SWAT-U with channel pruning improves validation accuracy on both ResNet-18 and DenseNet-121 while reducing training FLOPs by 3.3 \times .

ImageNet: Table 5 compares SWAT-U with channel pruning against four recent structured pruning algorithms. At 70% sparsity SWAT-U with channel pruning reduces training FLOPs by 3.19 \times by pruning 70% of the channels on ResNet50 while incurring only 1.2% loss in validation accuracy. SWAT-U with structured sparsity shows better accuracy but shows larger drops versus our baseline (trained with label smoothing) in some cases. The works we compare with start with a densely trained network, prune channels, then fine-tune and so increase training time contrary to our objective.

4.4 Sparse Accelerator Speedup

We believe SWAT is well suited for emerging sparse machine learning accelerator hardware designs like NVIDIA’s recently announced Ampere (A100) GPU. To estimate the speedup on a sparse accelerator, we have used an architecture simulator developed for a recent sparse accelerator hardware proposal [11]. The simulator counts only the effectual computation (non-zero computation) and exploits the sparsity present in the computation. The architecture has a 2D array of processing units where each processing unit has an array of multipliers and dedicated weight and activation and accumulation buffers. It counts the cycles taken to spatially map and schedules the computation present in each layer of the network. The memory hierarchy is similar to the DaDianNo architecture [7]. The activation and weight buffer can hold one entire layer at a time and hide the latency of memory transfer. The memory throughput is high enough to satisfy the computation throughput.

Table 6: Speedup due to SWAT on ML Accelerator

| Top- K Sparsity | Forward Pass Speed Up | Backward Pass Speed Up |
|-------------------|-----------------------|------------------------|
| 0% | 1× | 1× |
| 80% | 3.3× | 3.4× |
| 90% | 5.6× | 6.3× |

The simulator only implements the forward pass, and therefore the simulator does not simulate the backward pass. However, the backward pass convolution is a transposed convolution, which can be translated into a standard convolution by rotating the input tensor [16]. So we estimated the backward pass speedup by transforming transpose convolution into a standard convolution and using the inference simulator. Note, here the transformation overhead was not considered in the speedup. However, the overhead would be small in the actual hardware since this transformation operation is a simple rotation operation, i.e., rotating the tensor along some axis and, therefore, we assume it could be accelerated on hardware. Table 6 reports forward and backward pass training speedup (in simulated clock cycles) for SWAT-U with unstructured pruning on ResNet-50 with ImageNet. From Table 3 we see that at 80% sparsity SWAT-U incurs 1.63% accuracy loss but the data in Table 6 suggests it may improve training time by 3.3× on emerging platforms supporting supporting hardware acceleration of sparse computations.

4.5 Effect of updates to non-active weights

SWAT updates non-active weights in the backward pass using dense gradients and one might reasonable ask whether it would be possible to further decrease training time by masking these gradients. Figure 7 measures the effect of this masking on validation accuracy while training ResNet-18 on CIFAR-100. The data suggest it is important to update non-active weights. Since non-active weights are updated they may become active changing the topology. Figure 8 shows the effect of freezing the topology after differing number of epochs during training of ResNet18 on CIFAR100 dataset. Freezing topology exploration early is harmful to convergence and results in reduced final validation accuracy.

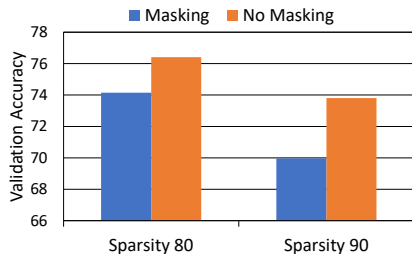


Figure 7: Effect of masking of gradient update for non-active weights.

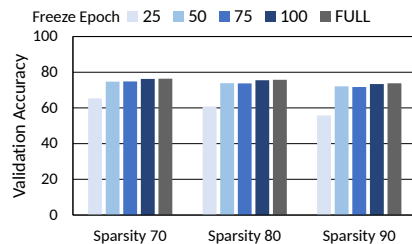


Figure 8: Effect of stopping dynamic topology exploration early.

5 Conclusion

In this work, we propose SWAT, a novel efficient training algorithm that sparsifies both the forward and the backward passes with negligible impact on convergence. SWAT is the first sparse learning algorithm we are aware of that can train both structured and unstructured sparse networks. SWAT achieves validation accuracy comparable to other pruning and sparse learning algorithms while demonstrating potential for significant reduction in training time on emerging platforms supporting hardware acceleration of sparse computations.

6 Broader Impact

This work has the following potential positive impact in society: 1) It is an entirely sparse training algorithm for emerging sparse hardware accelerators. 2) It makes training efficient and faster. Thus,

decreasing the model training cost. 3) It can reduce the overall carbon footprint of model training, which is a huge problem. Strubell et al. [57] shows that the carbon footprint of training models can release $5\times$ the carbon emission of a car during its lifetime. 4) It can enable us to train even bigger models, thus allowing us to achieve new state-of-the-art accuracies.

At the same time, this work may have some negative consequences because SWAT can enable us to develop better AI and better AI technologies may have negative societal implications such as strict surveillance, privacy concerns, and job loss.

7 Acknowledgements

We thank Francois Demoullin, Negar Goli, Dave Evans, Deval Shah, Yuan Hsi Chou, and the anonymous reviewers for their valuable comments on this work. This research has been funded in part by the Computing Hardware for Emerging Intelligent Sensory Applications (COHESA) project. COHESA is financed under the National Sciences and Engineering Research Council of Canada (NSERC) Strategic Networks grant number NETGP485577-15.

References

- [1] Tolu Alabi, Jeffrey D Blanchard, Bradley Gordon, and Russel Steinbach. Fast k-selection algorithms for graphics processing units. *Journal of Experimental Algorithmics (JEA)*, 17:4–1, 2012.
- [2] Jorge Albericio, Patrick Judd, Tayler Hetherington, Tor Aamodt, Natalie Enright Jerger, and Andreas Moshovos. Cnvlutin: Ineffectual-neuron-free deep neural network computing. *ACM SIGARCH Computer Architecture News*, 44(3):1–13, 2016.
- [3] Gene M Amdahl. Validity of the single processor approach to achieving large scale computing capabilities. In *Proceedings of the April 18-20, 1967, spring joint computer conference*, pages 483–485, 1967.
- [4] Manuel Blum, Robert W. Floyd, Vaughan Pratt, Ronald L. Rivest, and Robert E. Tarjan. Time bounds for selection. *Journal of Computer and System Sciences*, 7(4):448 – 461, 1973. ISSN 0022-0000. doi: [https://doi.org/10.1016/S0022-0000\(73\)80033-9](https://doi.org/10.1016/S0022-0000(73)80033-9). URL <http://www.sciencedirect.com/science/article/pii/S0022000073800339>.
- [5] Han Cai, Chuang Gan, Tianzhe Wang, Zhekai Zhang, and Song Han. Once-for-all: Train one network and specialize it for efficient deployment. In *International Conference on Learning Representations*, 2020.
- [6] Dongqu Chen, Guang-Zhong Sun, and Neil Zhenqiang Gong. Efficient approximate top-k query algorithm using cube index. In *Asia-Pacific Web Conference*, pages 155–167. Springer, 2011.
- [7] Yunji Chen, Tao Luo, Shaoli Liu, Shijin Zhang, Liqiang He, Jia Wang, Ling Li, Tianshi Chen, Zhiwei Xu, Ninghui Sun, et al. Dadiannao: A machine-learning supercomputer. In *2014 47th Annual IEEE/ACM International Symposium on Microarchitecture*, pages 609–622. IEEE, 2014.
- [8] Jungwook Choi, Pierce I-Jen Chuang, Zhuo Wang, Swagath Venkataramani, Vijayalakshmi Srinivasan, and Kailash Gopalakrishnan. Bridging the accuracy gap for 2-bit quantized neural networks (qnn). *arXiv preprint arXiv:1807.06964*, 2018.
- [9] Eric Chung, Jeremy Fowers, Kalin Ovtcharov, Michael Papamichael, Adrian Caulfield, Todd Massengill, Ming Liu, Daniel Lo, Shlomi Alkalay, Michael Haselman, et al. Serving dnns in real time at datacenter scale with project brainwave. *IEEE Micro*, 38(2):8–20, 2018.
- [10] Dipankar Das, Naveen Mellempudi, Dheevatsa Mudigere, Dhiraj Kalamkar, Sasikanth Avancha, Kunal Banerjee, Srinivas Sridharan, Karthik Vaidyanathan, Bharat Kaul, Evangelos Georganas, Alexander Heinecke, Pradeep Dubey, Jesus Corbal, Nikita Shustrov, Roma Dubtsov, Evarist Fomenko, and Vadim Pirogov. Mixed precision training of convolutional neural networks using integer operations. In *International Conference on Learning Representations*, 2018. URL <https://openreview.net/forum?id=H135uzZ0->.

- [11] Alberto Delmas Lascorz, Patrick Judd, Dylan Malone Stuart, Zissis Poulos, Mostafa Mahmoud, Sayeh Sharify, Milos Nikolic, Kevin Siu, and Andreas Moshovos. Bit-tactical: A software/hardware approach to exploiting value and bit sparsity in neural networks. In *Proceedings of the Twenty-Fourth International Conference on Architectural Support for Programming Languages and Operating Systems*, pages 749–763, 2019.
- [12] Tim Dettmers and Luke Zettlemoyer. Sparse networks from scratch: Faster training without losing performance. *arXiv preprint arXiv:1907.04840*, 2019.
- [13] Xiaohan Ding, Guiguang Ding, Yuchen Guo, Jungong Han, and Chenggang Yan. Approximated oracle filter pruning for destructive cnn width optimization. *arXiv preprint arXiv:1905.04748*, 2019.
- [14] Chao Dong, Chen Change Loy, Kaiming He, and Xiaoou Tang. Learning a deep convolutional network for image super-resolution. In *European conference on computer vision*, pages 184–199. Springer, 2014.
- [15] John Duchi, Elad Hazan, and Yoram Singer. Adaptive subgradient methods for online learning and stochastic optimization. *Journal of machine learning research*, 12(Jul):2121–2159, 2011.
- [16] Vincent Dumoulin and Francesco Visin. A guide to convolution arithmetic for deep learning. *arXiv preprint arXiv:1603.07285*, 2016.
- [17] Utku Evci, Trevor Gale, Jacob Menick, Pablo Samuel Castro, and Erich Elsen. Rigging the lottery: Making all tickets winners, 2019.
- [18] Georgios Georgiadis. Accelerating convolutional neural networks via activation map compression. In *Proceedings of the IEEE Conference on Computer Vision and Pattern Recognition*, pages 7085–7095, 2019.
- [19] Negar Goli and Tor Aamodt. Resprop: Reuse sparsified backpropagation. In *Proceedings of the IEEE Conference on Computer Vision and Pattern Recognition*, 2020.
- [20] Maximilian Golub, Guy Lemieux, and Mieszko Lis. Full deep neural network training on a pruned weight budget. *arXiv preprint arXiv:1806.06949*, 2018.
- [21] Song Han, Huizi Mao, and William J Dally. Deep compression: Compressing deep neural networks with pruning, trained quantization and huffman coding. *arXiv preprint arXiv:1510.00149*, 2015.
- [22] Kaiming He, Xiangyu Zhang, Shaoqing Ren, and Jian Sun. Deep residual learning for image recognition. In *Proceedings of the IEEE conference on computer vision and pattern recognition*, pages 770–778, 2016.
- [23] Yang He, Guoliang Kang, Xuanyi Dong, Yanwei Fu, and Yi Yang. Soft filter pruning for accelerating deep convolutional neural networks. In *Proceedings of the 27th International Joint Conference on Artificial Intelligence*, pages 2234–2240. AAAI Press, 2018.
- [24] Yihui He, Xiangyu Zhang, and Jian Sun. Channel pruning for accelerating very deep neural networks. In *Proceedings of the IEEE International Conference on Computer Vision*, pages 1389–1397, 2017.
- [25] C. A. R. Hoare. Algorithm 65: Find. *Commun. ACM*, 4(7):321–322, July 1961. ISSN 0001-0782. doi: 10.1145/366622.366647. URL <http://doi.acm.org/10.1145/366622.366647>.
- [26] Gao Huang, Zhuang Liu, Laurens Van Der Maaten, and Kilian Q Weinberger. Densely connected convolutional networks. In *Proceedings of the IEEE conference on computer vision and pattern recognition*, pages 4700–4708, 2017.
- [27] Sergey Ioffe and Christian Szegedy. Batch normalization: Accelerating deep network training by reducing internal covariate shift. *arXiv preprint arXiv:1502.03167*, 2015.

- [28] Norman P Jouppi, Cliff Young, Nishant Patil, David Patterson, Gaurav Agrawal, Raminder Bajwa, Sarah Bates, Suresh Bhatia, Nan Boden, Al Borchers, et al. In-datacenter performance analysis of a tensor processing unit. In *Proceedings of the 44th Annual International Symposium on Computer Architecture*, pages 1–12, 2017.
- [29] Diederik P Kingma and Jimmy Ba. Adam: A method for stochastic optimization. *arXiv preprint arXiv:1412.6980*, 2014.
- [30] Alex Krizhevsky, Ilya Sutskever, and Geoffrey E Hinton. Imagenet classification with deep convolutional neural networks. In *Advances in neural information processing systems*, pages 1097–1105, 2012.
- [31] Alex Krizhevsky et al. Learning multiple layers of features from tiny images. Technical report, Citeseer, 2009.
- [32] Mark Kurtz, Justin Kopinsky, Rati Gelashvili, Alexander Matveev, John Carr, Michael Goin, William Leiserson, Sage Moore, Bill Nell, Nir Shavit, et al. Inducing and exploiting activation sparsity for fast neural network inference.
- [33] Aditya Kusupati, Vivek Ramanujan, Raghav Somani, Mitchell Wortsman, Prateek Jain, Sham Kakade, and Ali Farhadi. Soft threshold weight reparameterization for learnable sparsity. *arXiv preprint arXiv:2002.03231*, 2020.
- [34] Yann LeCun, John S Denker, and Sara A Solla. Optimal brain damage. In *Advances in neural information processing systems*, pages 598–605, 1990.
- [35] Hao Li, Asim Kadav, Igor Durdanovic, Hanan Samet, and Hans Peter Graf. Pruning filters for efficient convnets. *arXiv preprint arXiv:1608.08710*, 2016.
- [36] Junjie Liu, Zhe XU, Runbin SHI, Ray C. C. Cheung, and Hayden K.H. So. Dynamic sparse training: Find efficient sparse network from scratch with trainable masked layers. In *International Conference on Learning Representations*, 2020. URL <https://openreview.net/forum?id=SJ1bgJrtDB>.
- [37] Liu Liu, Lei Deng, Xing Hu, Maohua Zhu, Guoqi Li, Yufei Ding, and Yuan Xie. Dynamic sparse graph for efficient deep learning. In *International Conference on Learning Representations*, 2019. URL <https://openreview.net/forum?id=H1goBoR9F7>.
- [38] Zhuang Liu, Jianguo Li, Zhiqiang Shen, Gao Huang, Shoumeng Yan, and Changshui Zhang. Learning efficient convolutional networks through network slimming. In *Proceedings of the IEEE International Conference on Computer Vision*, pages 2736–2744, 2017.
- [39] Christos Louizos, Max Welling, and Diederik P Kingma. Learning sparse neural networks through l_0 regularization. *arXiv preprint arXiv:1712.01312*, 2017.
- [40] Jian-Hao Luo, Jianxin Wu, and Weiyao Lin. Thinet: A filter level pruning method for deep neural network compression. In *Proceedings of the IEEE international conference on computer vision*, pages 5058–5066, 2017.
- [41] Huizi Mao, Song Han, Jeff Pool, Wenshuo Li, Xingyu Liu, Yu Wang, and William J Dally. Exploring the regularity of sparse structure in convolutional neural networks. *arXiv preprint arXiv:1705.08922*, 2017.
- [42] Decebal Constantin Mocanu, Elena Mocanu, Peter Stone, Phuong H Nguyen, Madeleine Gibescu, and Antonio Liotta. Scalable training of artificial neural networks with adaptive sparse connectivity inspired by network science. *Nature communications*, 9(1):2383, 2018.
- [43] Dmitry Molchanov, Arsenii Ashukha, and Dmitry Vetrov. Variational dropout sparsifies deep neural networks. In *Proceedings of the 34th International Conference on Machine Learning-Volume 70*, pages 2498–2507. JMLR. org, 2017.
- [44] Pavlo Molchanov, Stephen Tyree, Tero Karras, Timo Aila, and Jan Kautz. Pruning convolutional neural networks for resource efficient inference. *arXiv preprint arXiv:1611.06440*, 2016.

- [45] Hesham Mostafa and Xin Wang. Parameter efficient training of deep convolutional neural networks by dynamic sparse reparameterization. In *International Conference on Machine Learning*, pages 4646–4655, 2019.
- [46] David R. Musser. Introspective sorting and selection algorithms. *Software: Practice and Experience*, 27(8):983–993, 1997. doi: 10.1002/(SICI)1097-024X(199708)27:8<983::AID-SPE117>3.0.CO;2-#. URL <https://onlinelibrary.wiley.com/doi/abs/10.1002/%28SICI%291097-024X%28199708%2927%3A8%3C983%3A%3AAID-SPE117%3E3.0.CO%3B2-%23>.
- [47] NVIDIA Corporation. NVIDIA Turing Architecture Whitepaper. <https://www.nvidia.com/content/dam/en-zz/Solutions/design-visualization/technologies/turing-architecture/NVIDIA-Turing-Architecture-Whitepaper.pdf>, June 2017.
- [48] NVIDIA Corporation. NVIDIA TESLA V100 GPU ARCHITECTURE. <http://images.nvidia.com/content/volta-architecture/pdf/volta-architecture-whitepaper.pdf>, June 2017.
- [49] NVIDIA Corporation. NVIDIA A100 Tensor Core GPU Architecture. <https://www.nvidia.com/content/dam/en-zz/Solutions/Data-Center/nvidia-ampere-architecture-whitepaper.pdf>, May 2020.
- [50] Angshuman Parashar, Minsoo Rhu, Anurag Mukkara, Antonio Puglielli, Rangharajan Venkatesan, Brucek Khailany, Joel Emer, Stephen W Keckler, and William J Dally. Scnn: An accelerator for compressed-sparse convolutional neural networks. In *2017 ACM/IEEE 44th Annual International Symposium on Computer Architecture (ISCA)*, pages 27–40. IEEE, 2017.
- [51] Adam Paszke, Sam Gross, Soumith Chintala, Gregory Chanan, Edward Yang, Zachary DeVito, Zeming Lin, Alban Desmaison, Luca Antiga, and Adam Lerer. Automatic differentiation in pytorch. 2017.
- [52] Hanyu Peng, Jiaxiang Wu, Shifeng Chen, and Junzhou Huang. Collaborative channel pruning for deep networks. In *International Conference on Machine Learning*, pages 5113–5122, 2019.
- [53] Shaoqing Ren, Kaiming He, Ross Girshick, and Jian Sun. Faster r-cnn: Towards real-time object detection with region proposal networks. In C. Cortes, N. D. Lawrence, D. D. Lee, M. Sugiyama, and R. Garnett, editors, *Advances in Neural Information Processing Systems 28*, pages 91–99. Curran Associates, Inc., 2015.
- [54] Minsoo Rhu, Mike O’Connor, Niladrish Chatterjee, Jeff Pool, Youngeun Kwon, and Stephen W Keckler. Compressing dma engine: Leveraging activation sparsity for training deep neural networks. In *2018 IEEE International Symposium on High Performance Computer Architecture (HPCA)*, pages 78–91. IEEE, 2018.
- [55] Anil Shanbhag, Holger Pirk, and Samuel Madden. Efficient top-k query processing on massively parallel hardware. In *Proceedings of the 2018 International Conference on Management of Data*, pages 1557–1570, 2018.
- [56] Karen Simonyan and Andrew Zisserman. Very deep convolutional networks for large-scale image recognition. *arXiv preprint arXiv:1409.1556*, 2014.
- [57] Emma Strubell, Ananya Ganesh, and Andrew McCallum. Energy and policy considerations for deep learning in nlp. *arXiv preprint arXiv:1906.02243*, 2019.
- [58] Xu Sun, Xuancheng Ren, Shuming Ma, and Houfeng Wang. meprop: Sparsified back propagation for accelerated deep learning with reduced overfitting. In *Proceedings of the 34th International Conference on Machine Learning-Volume 70*, pages 3299–3308. JMLR. org, 2017.
- [59] Christian Szegedy, Alexander Toshev, and Dumitru Erhan. Deep neural networks for object detection. In C. J. C. Burges, L. Bottou, M. Welling, Z. Ghahramani, and K. Q. Weinberger, editors, *Advances in Neural Information Processing Systems 26*, pages 2553–2561. Curran Associates, Inc., 2013. URL <http://papers.nips.cc/paper/5207-deep-neural-networks-for-object-detection.pdf>.

- [60] Christian Szegedy, Wei Liu, Yangqing Jia, Pierre Sermanet, Scott Reed, Dragomir Anguelov, Dumitru Erhan, Vincent Vanhoucke, and Andrew Rabinovich. Going deeper with convolutions. In *Proceedings of the IEEE conference on computer vision and pattern recognition*, pages 1–9, 2015.
- [61] Christian Szegedy, Vincent Vanhoucke, Sergey Ioffe, Jon Shlens, and Zbigniew Wojna. Rethinking the inception architecture for computer vision. In *Proceedings of the IEEE conference on computer vision and pattern recognition*, pages 2818–2826, 2016.
- [62] Naigang Wang, Jungwook Choi, Daniel Brand, Chia-Yu Chen, and Kailash Gopalakrishnan. Training deep neural networks with 8-bit floating point numbers. In *Advances in neural information processing systems*, pages 7675–7684, 2018.
- [63] Bingzhen Wei, Xu Sun, Xuancheng Ren, and Jingjing Xu. Minimal effort back propagation for convolutional neural networks. *arXiv preprint arXiv:1709.05804*, 2017.
- [64] Wei Wen, Chunpeng Wu, Yandan Wang, Yiran Chen, and Hai Li. Learning structured sparsity in deep neural networks. In *Advances in neural information processing systems*, pages 2074–2082, 2016.
- [65] Jiaxiang Wu, Cong Leng, Yuhang Wang, Qinghao Hu, and Jian Cheng. Quantized convolutional neural networks for mobile devices. In *Proceedings of the IEEE Conference on Computer Vision and Pattern Recognition*, pages 4820–4828, 2016.
- [66] Shuang Wu, Guoqi Li, Feng Chen, and Luping Shi. Training and inference with integers in deep neural networks. In *International Conference on Learning Representations*, 2018. URL <https://openreview.net/forum?id=HJGXzmspb>.
- [67] Sergey Zagoruyko and Nikos Komodakis. Wide residual networks. *arXiv preprint arXiv:1605.07146*, 2016.
- [68] Kai Zhang, Wangmeng Zuo, Shuhang Gu, and Lei Zhang. Learning deep cnn denoiser prior for image restoration. In *Proceedings of the IEEE conference on computer vision and pattern recognition*, pages 3929–3938, 2017.
- [69] Shijin Zhang, Zidong Du, Lei Zhang, Huiying Lan, Shaoli Liu, Ling Li, Qi Guo, Tianshi Chen, and Yunji Chen. Cambricon-x: An accelerator for sparse neural networks. In *The 49th Annual IEEE/ACM International Symposium on Microarchitecture*, page 20. IEEE Press, 2016.
- [70] Shuchang Zhou, Yuxin Wu, Zekun Ni, Xinyu Zhou, He Wen, and Yuheng Zou. Dorefa-net: Training low bitwidth convolutional neural networks with low bitwidth gradients. *arXiv preprint arXiv:1606.06160*, 2016.
- [71] Michael Zhu and Suyog Gupta. To prune, or not to prune: exploring the efficacy of pruning for model compression. *arXiv preprint arXiv:1710.01878*, 2017.
- [72] Zhuangwei Zhuang, Mingkui Tan, Bohan Zhuang, Jing Liu, Yong Guo, Qingyao Wu, Junzhou Huang, and Jinhui Zhu. Discrimination-aware channel pruning for deep neural networks. In *Advances in Neural Information Processing Systems*, pages 875–886, 2018.

Appendix A Appendix

A.1 Detailed description of the SWAT algorithm

The SWAT algorithm is summarized in Algorithm 1. The shaded region represents the sparse computation step which could be exploited on sparse machine learning accelerators. The SWAT algorithm consists of three parts: Forward Computation, Backward Computation, and the Parameter Update.

The forward computation (Line 1 to 1) for each layer proceeds as follows: First, we check if the current layer is a convolutional or fully-connected layer (Line 1). If neither, perform the regular (non-SWAT) forward pass computation (Line 1) and save dense weights and activations (Line 1).

Algorithm 1 SWAT Algorithm

The data: Training iteration t and Top- K sampling period P . Network with L layers and previous weight parameters \mathbf{w}^t . Sparsity distribution algorithm D . Mini-batch of inputs (\mathbf{a}_0) and corresponding targets (\mathbf{a}^*). Learning rate η . Gradient descent optimization algorithm *Optimizer*.

The result: Updated weight parameters \mathbf{w}^{t+1} .

Stage 1. Forward Computation

```
for  $l = 1$  to  $L$  do
  if  $l$  is a convolutional or fully-connected layer then
    if  $t \bmod P = 0$  then
       $S_l \leftarrow \text{getLayerSparsity}(l, D)$ 
       $t_l^w \leftarrow \text{getThreshold}(\mathbf{w}_l, S_l, t)$ 
       $t_l^a \leftarrow \text{getThreshold}(\mathbf{a}_{l-1}, S_l, t)$ 
    end
     $\mathbf{W}_l^t \leftarrow f_{TOPK}(\mathbf{w}_l^t, t_l^w)$ 
     $\mathbf{a}_l^t \leftarrow \text{forward}(\mathbf{W}_l^t, \mathbf{a}_{l-1}^t)$ 
     $\mathbf{a}_{l-1}^t \leftarrow f_{TOPK}(\mathbf{a}_{l-1}^t, t_l^a)$ 
    save_for_backward $_l \leftarrow \mathbf{W}_l^t, \mathbf{a}_{l-1}$ 
  else
     $\mathbf{a}_l \leftarrow \text{forward}(\mathbf{w}_l^t, \mathbf{a}_{l-1})$ 
    save_for_backward $_l \leftarrow \mathbf{w}_l^t, \mathbf{a}_{l-1}$ 
  end
end
```

Stage 2. Backward Computation

Compute the gradient of the output layer $\nabla_{\mathbf{a}_L} = \frac{\partial \text{loss}(\mathbf{a}_L, \mathbf{a}^*)}{\partial \mathbf{a}_L}$

```
for  $l = L$  to  $1$  do
   $\mathbf{W}_l^t, \mathbf{a}_{l-1} \leftarrow \text{save\_for\_backward}_l$ 
  if  $l$  is a convolutional or fully-connected layer then
     $\nabla_{\mathbf{a}_{l-1}} \leftarrow \text{backward\_input}(\nabla_{\mathbf{a}_l}, \mathbf{W}_l^t)$ 
     $\nabla_{\mathbf{w}_{l-1}} \leftarrow \text{backward\_weight}(\nabla_{\mathbf{a}_l}, \mathbf{a}_{l-1}^t)$ 
  else
     $\nabla_{\mathbf{a}_{l-1}} \leftarrow \text{backward\_input}(\nabla_{\mathbf{a}_l}, \mathbf{W}_l^t)$ 
     $\nabla_{\mathbf{w}_{l-1}} \leftarrow \text{backward\_weight}(\nabla_{\mathbf{a}_l}, \mathbf{a}_{l-1}^t)$ 
  end
end
```

Stage 3. Parameter Update

```
for  $l = 1$  to  $L$  do
   $\mathbf{w}_l^{t+1} \leftarrow \text{Optimizer}(\mathbf{w}_l^t, \nabla_{\mathbf{w}_l}, \eta)$ 
end
```

Otherwise, if the training iteration t is a multiple of the Top- K sampling period P then we obtain the target sparsity \mathbf{S}_l of layer l based upon distribution algorithm D (Line 1) where D is one of the techniques described in Section 3.3.2. Then, we compute threshold t^w for weight sparsity (Line 1) used in the forward pass and threshold t^a for use in sparsifying activations prior to saving to memory for use in the the backward pass (Line 1). Prior to performing the forward computation (Line 1) we compute the active weights \mathbf{W}_l^t by applying the sparsifying function, f_{TOPK} using threshold t^w . For input tensor \mathbf{x}_i For fine-grained sparsity $f_{TOPK}(\mathbf{x}, t)$ maps input elements $x_i \in \mathbf{x}$ to output elements y_i according to:

$$y_i = \begin{cases} 0, & |x_i| \leq t \\ x_i, & \text{otherwise} \end{cases}$$

For coarse-grained sparsity (Section 3.3.1), which we apply only to weights, $f_{TOPK}(\mathbf{x}, t)$ maps input elements $x_i \in \mathbf{x}$ to output elements y_i where i is an element of channel C according to:

$$y_i = \begin{cases} 0, & \sum_{i \in C} |x_i| \leq t \\ x_i, & \text{otherwise} \end{cases}$$

Next, we perform sparse forward computations, `forward`, corresponding to Equation 1 in the paper to generate output activation (Line 1). Next, we apply fine-grained Top- K sparsification to the input activations (Line 1). Save sparse active weight parameters \mathbf{W}_l^t and input activations \mathbf{a}_{l-1} for the backward pass (Line 1).

After the forward pass the loss function is applied and the back propagated error-gradient for the output layer is computed (Line 1). Then, the backward pass computation (Line 1 to 1) proceeds as follows: First, we load the saved parameters and input activations of the current layer (Line 1). Next, we perform the backward pass to generate the input activation gradients and weight gradients using `backward_input` and `backward_weight` functions, which correspond to Equations 2 and 3 in the paper, respectively. As sparse input activations and parameters are saved in the forward pass the computation is sparse.

After the backward pass of the current mini-batch, the optimizer uses the computed weight gradients to update the parameters (Line 1 to 1).

A.2 CIFAR-100

A.2.1 Unstructured SWAT

Table 7 compares SWAT-U, SWAT-ERK and SWAT-M with unstructured sparsity for VGG-16, WRN-16-8 and DenseNet-121 architecture on CIFAR-100 dataset. The training procedure is the same as outlined in Section 4.1 in the paper. Hyperparameters are listed in Appendix subsection A.10.

Table 7: Unstructured SWAT on CIFAR-100 dataset.

| Network | Methods | Training Sparsity | | Top-1 | |
|--------------|----------|-------------------|----------------|--------------|-----------------|
| | | Weight (%) | Activation (%) | Accuracy (%) | Accuracy Change |
| VGG-16 | SWAT-U | 90.0 | 90.0 | 69.8 | -2.3 |
| | SWAT-ERK | 90.0 | 69.6 | 71.8 | -0.3 |
| | SWAT-M | 90.0 | 59.9 | 72.2 | +0.1 |
| WRN-16-8 | SWAT-U | 90.0 | 90.0 | 77.6 | -1.7 |
| | SWAT-ERK | 90.0 | 77.6 | 78.5 | -0.8 |
| | SWAT-M | 90.0 | 73.3 | 77.9 | -1.4 |
| DENSENET-121 | SWAT-U | 90.0 | 90.0 | 77.2 | -0.4 |
| | SWAT-ERK | 90.0 | 90.0 | 76.5 | -1.1 |
| | SWAT-M | 90.0 | 84.2 | 75.5 | -2.1 |

A.2.2 Structured SWAT

Table 8 compares SWAT-U with unstructured sparsity for ResNet-18 and DenseNet-121 architecture on CIFAR-100 dataset. The training procedure is the same as outlined in Section 4.1 in the paper. Hyperparameters are listed in Appendix subsection A.10.

Table 8: Structured SWAT on CIFAR-100 dataset.

| Network | Methods | Training Sparsity | | | Top-1 | |
|--------------|---------|-------------------|----------------|--------------------|--------------|-----------------|
| | | Weight (%) | Activation (%) | Channel Pruned (%) | Accuracy (%) | Accuracy Change |
| RESNET-18 | SWAT-U | 50.0 | 50.0 | 50.0 | 76.4 | -0.4 |
| | | 60.0 | 60.0 | 60.0 | 76.2 | -0.6 |
| | | 70.0 | 70.0 | 70.0 | 75.6 | -1.2 |
| DENSENET-121 | SWAT-U | 50.0 | 50.0 | 50.0 | 78.7 | +0.9 |
| | | 60.0 | 60.0 | 60.0 | 78.5 | +0.4 |
| | | 70.0 | 70.0 | 70.0 | 78.1 | +0.3 |

A.3 FLOP Calculation

Consider a convolution layer with input tensor $X \in \mathbb{R}^{N \times C \times X \times Y}$ and weight tensor $W \in \mathbb{R}^{F \times C \times R \times S}$ to produce output tensor $O \in \mathbb{R}^{N \times F \times H \times W}$. Input tensor has N samples; each sample has C input channels of dimension $X \times Y$. Weight tensor has F filters and each filters has C channels of dimension $R \times S$. Output tensor has N output samples and each sample has F output channels of dimension $H \times W$.

During the forward pass, input tensor is convolved with weight tensor to produce output tensor. In contrast, in the backward pass, the error-gradient of output tensor is deconvolved with input and weight tensor to produce weight gradient and input gradient respectively. The forward pass FLOP calculation assumes $s1$ sparsity in weight tensor. The effect of default sparsity in activation for forward pass computation is ignored since the default activation sparsity is present for both sparse learning and SWAT algorithms. However, for the backward pass FLOP calculation, since for SWAT the activation is explicitly sparsified therefore the FLOP calculation for SWAT is done using $s1$ weight sparsity and $s2$ activation sparsity whereas for sparse learning algorithms, $s1$ weight sparsity and default activation sparsity is assumed. The default activation sparsity generally vary between 30 – 50%, for our calculation we assumed default activation sparsity of 50%.

All the sparse learning algorithms and SWAT require some extra FLOP for connectivity update and regrowth connection such as dropping low magnitude component and thresholding. We omit the FLOP needed for these operations in our training FLOP calculation. For dynamic sparse learning algorithms such as SNFS [12], DSR [45] and DST [36], the weight sparsity varies during iterations and therefore we computed the average weight sparsity for different layers during the entire training and used it for computing the training FLOP.

A.3.1 Computation in Convolution Layer

Forward Pass

Filter from the weight tensor is convolved with some sub-volume of input tensor of dimension $X^{sub} \in \mathbb{R}^{C \times R \times S}$ to produce a single value in output tensor. Therefore, the total FLOP for any single value in output tensor is $C \times R \times S$ floating-point multiplication + $C \times R \times S - 1$ floating-point addition. This is approximately equal to $C \times R \times S$ floating-point MAC operations. Note, here 1 floating-point MAC operations = 1 floating-point multiplication + 1 floating-point addition. Thus, the total computation in the forward pass is equal to $(C \times R \times S) \times N \times F \times H \times W$ MAC operations.

Now, lets assume weight tensor is sparse. The overall sparsity in the weight tensor is $s1$ and the sparsity per filter in the weight tensor is s^1, s^2, \dots, s^F , for F filters in the layer. Note, $s1 = \frac{\sum_{x=1}^F s^x}{F}$. Theoretically only the non-zero weight will contribute to the FLOP. Therefore, the total FLOP for a single value in output tensor produce by the filter x is $s^x \times C \times R \times S$ MAC operations. Thus, the total FLOP contribution for producing an output channel, of dimension $H \times W$, by the filter x is $s^x \times (C \times R \times S) \times H \times W$. Therefore, the total FLOP for N input batches and F output channel is equal to $\sum_{x=1}^F (s^x \times (C \times R \times S) \times N \times H \times W) = (\sum_{x=1}^F s^x) \times (C \times R \times S) \times N \times H \times W = s1 \times F \times (C \times R \times S) \times N \times H \times W$. Hence, theoretically the FLOP reduction is proportional to sparsity in weight tensor.

$$\text{Forward Pass FLOP} = s1 \times F \times (C \times R \times S) \times N \times H \times W. \quad (4)$$

Backward Pass

For the backward pass, we back-propagate the error signal for computing the gradient of parameters. During the backward pass, each layer calculates 2 quantities: input gradient and weight gradient.

For the input gradient computation, the output gradient is deconvolved with filters to produce the input gradient. It can be implemented by rotating the filter tensor from $W \in \mathbb{R}^{F \times C \times R \times S}$ to $\tilde{W} \in \mathbb{R}^{C \times F \times R \times S}$ and convolving with output gradient. In this computation, the convolution data is output gradient and convolution kernels are filters. Therefore, as described in the previous section, the total MAC in the input gradient is approximately proportional to $(F \times R \times S) \times N \times C \times X \times Y$. Hence, the FLOP reduction with sparsity $s1$ in weight tensor will be approximately proportional to $s1 \times C \times (F \times R \times S) \times N \times X \times Y$.

$$\text{Input Gradient FLOP} = s1 \times C \times (F \times R \times S) \times N \times X \times Y. \quad (5)$$

For the weight gradient computation, the input activation is deconvolved with the output gradient to produce the weight gradient. It can be implemented by rotating the output gradient tensor from $\nabla O \in \mathbb{R}^{N \times F \times H \times W}$ to $\tilde{\nabla O} \in \mathbb{R}^{F \times N \times H \times W}$ and input activation from $X \in \mathbb{R}^{N \times C \times X \times Y}$ to $\tilde{X} \in \mathbb{R}^{C \times N \times X \times Y}$. The rotated output gradient is convolved on input activation to produce weight gradient. In this computation, the convolution data is input activation and convolution kernel is output gradient. Therefore, the total MAC in the weight gradient is approximately proportional to $(N \times X \times Y) \times F \times C \times R \times S$. Hence, as described in the previous section, the FLOP reduction with sparsity $s2$ in input activation tensor will be approximately proportional to $s2 \times (N \times X \times Y) \times F \times C \times R \times S$.

$$\text{Weight Gradient FLOP} = s2 \times (N \times X \times Y) \times F \times C \times R \times S. \quad (6)$$

Thus, the computational expense of the backward pass is approximately twice that of forward pass.

A.3.2 Computation in Linear Layer

Consider a linear layer with input tensor $X \in \mathbb{R}^{N \times X}$ and weight tensor $W \in \mathbb{R}^{X \times Y}$ to produce output tensor $O \in \mathbb{R}^{N \times Y}$. During the forward pass, input tensor is multiplied with weight tensor to produce output tensor. In contrast, in the backward pass, the error-gradient of output tensor is multiplied with input and weight tensor to produce error-gradient of weight and error-gradient input tensor.

Forward Pass

The total FLOP for the forward pass is $N \times Y \times X$ floating-point multiplication + $N \times Y \times (X - 1)$ floating-point addition. This is approximately equal to $N \times X \times Y$ floating-point MAC operations.

Now, let's assume weight tensor is sparse. The overall sparsity in the weight tensor is s and the sparsity per column in the weight tensor is s^1, s^2, \dots, s^Y for Y columns in the weight tensor. Note, $s = \frac{\sum_{y=1}^Y s^y}{Y}$. Theoretically only the non-zero weight will contribute to the FLOP. Therefore, the total FLOP for a single value in the y column of output tensor is $s^y \times X$ MAC operations. Thus, the total FLOP for all the element in the y column of output tensor is $s^y \times X \times N$. Therefore, the FLOP in forward pass is equal to $\sum_{y=1}^Y s^y \times N \times Y = N \times X \times (\sum_{x=1}^F s^x) = s \times N \times X \times Y$. Thus, theoretically the FLOP reduction will be proportional to sparsity in weight tensor.

Backward Pass

The computational expense of the backward pass is twice that of forward pass and is reduced proportionally to the sparsity of weight and activation tensor.

A.4 Top-K Overhead

The Top-K operation can be efficiently implemented by finding the K-th largest element using an introselect algorithm and performing thresholding operation over the tensor. To estimate the overhead of finding the K-th largest element, we use `numpy.partition` function. The `numpy.partition` function uses the introselect algorithm and rearranges the array such that the element in the K-th position is in the position it would be in the sorted array. This overhead would be larger than the cost of finding the K-th largest element due to the extra rearrangement operations and thus serves as an upper bound on Top-K overhead.

We profile the numpy partition function using Vtune 2020.1.0.607630 on Intel(R) Core(TM) i9-7920X CPU @ 2.90GHz. Table 9 shows the total number of retired instruction while executing numpy.partition for different array size. We can observe that the overhead of the numpy.partition increases linearly with array size.

Table 9: Overhead of computing the K-th largest element using introselect algorithm

| Array Size | Retired Instruction | Retired Instruction/Size |
|------------|---------------------|--------------------------|
| 1000 | 15215 | 15.2 |
| 10000 | 217863 | 21.8 |
| 100000 | 1381744 | 13.8 |
| 1000000 | 12454369 | 12.6 |

The Top-K function in Pytorch framework is not an optimized implementation for GPU. Therefore, to estimate the Top-K overhead on GPU, we used the efficient Radix based Top-K implementation by Shanbhag et al. [55]. Table 10 shows the overall overhead of performing the Top-K operation for ResNet-50 on the ImageNet dataset with a batch-size of 32 on NVIDIA RTX-2080 Ti.

Table 10: Top-K Overhead

| Top-K Weight | Top-K Activation | Forward + Backward Pass | Total Top-K Overhead |
|--------------|------------------|-------------------------|----------------------|
| 18 ms | 452 ms | 147 ms | 470 ms |

SWAT-U reduces the training FLOP per iteration by 76.1% and 85.6% at 80% and 90% sparsity respectively. Therefore, theoretical training speed up (assuming hardware can directly translate FLOPs reduction into reduced execution time) for the SWAT-U algorithm with a Top-K operation of 1000 iteration, at 80%, and 90% sparsity would be $4.13\times$ and $6.79\times$ respectively. These numbers are found as follows:

$$\text{Speed Up at 80\% sparsity} = \frac{1000 \times 147}{999 \times (1 - 0.761) \times 147 + 147 \times (1 - 0.761) + 470} = 4.13 \quad (7)$$

$$\text{Speed Up at 90\% sparsity} = \frac{1000 \times 147}{999 \times (1 - 0.856) \times 147 + 147 \times (1 - 0.856) + 470} = 6.79 \quad (8)$$

There are additional optimizations that could potentially be applied to further reduce the Top-K overhead which we have not yet evaluated: (1) The overhead reported in Table 10 is for a Top-K operation, whereas we only need to find a threshold, not the top-K weights or activation values and then we can use that threshold for many iterations as suggested by the data in Figure 4 in the paper. So a more efficient implementation should be possible using the K-Selection Algorithm for which efficient GPU implementations have been proposed [1]; (2) There are more efficient *approximate* Top-K algorithms [6]; (3) Given a slow rate of change in threshold values per iteration, we could potentially **hide** the latency of the Top-K or K-Selection operation during the longer Top-K sampling period by starting the operation earlier. I.e., we can potentially exploit the stability in thresholds to move obtaining computation of updates to thresholds (after the first iteration) from the critical path; (4) The overhead of finding the Top-K operation on activations in Table 10 is higher due to large activation size. We speculate this overhead could be reduced significantly by performing the Top-K operation on activation for a single sample and using the resulting threshold for computing the approximate Top-K operation for the entire batch.

A.5 Top-K Selection

Given CNNs operate on tensors with many dimensions, there are several options for how to select which components are set to zero during sparsification. Our CNNs operate on fourth-order tensors, $T \in R^{N \times C \times H \times W}$. Below we evaluate three variants of the Top-K operation illustrated in the right side of Figure 9. We also compared against a null hypothesis in which randomly selected components of a tensor are set to zero.

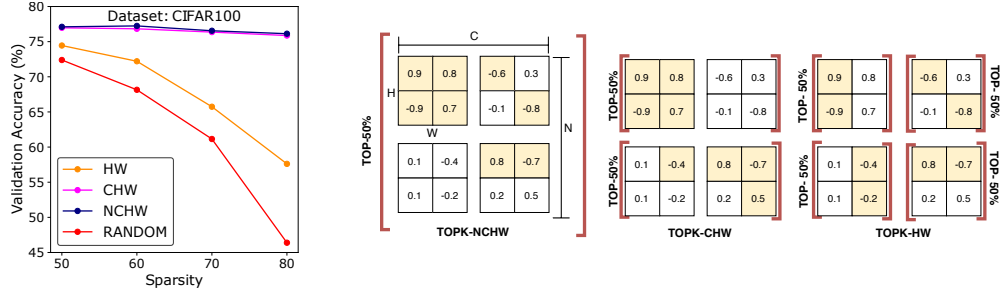


Figure 9: **Different ways of performing top-k operation.** ‘N’ denotes the #samples in the mini-batch or filters in the layer, ‘C’ denotes the #channels in the layer. ‘H’ and ‘W’ denote the height and width of the filter/activation map in the layer. Color represent the selected activations/weights by the Top-K operation.

The first variant, labeled TOPK-NCHW in Figure 9, selects activations and weights to set to zero by considering the entire mini-batch. This variant performs Top-K operation over the entire tensor, $f_{TOPK}^{\{N,C,H,W\}}(T)$, where the superscript represents the dimension along which the Top-K operation is performed. The second variant (TOPK-CHW) performs Top-K operation over the dimensions C, H and W i.e., $f_{TOPK}^{\{C,H,W\}}(T)$, i.e., selects $K\%$ of input activations from every mini-batch sample and $K\%$ of weights from every filter in the layer. The third variant (TOPK-HW) is the strictest form of Top-K operation. It select $K\%$ of activations or weights from all channels, and thereby performing the Top-K operation over the dimension H and W , i.e., $f_{TOPK}^{\{H,W\}}(T_{H,W})$.

The left side of Figure 9 shows the accuracy achieved on ResNet-18 for CIFAR100 when using SAW (see Appendix A.7) configured with each of these Top-K variants along with a variant where a random subset of components is set to zero. The results show, first, that randomly selecting works only for low sparsity. At high sparsity all variants of Top-K outperform random selection by a considerable margin. Second, they show that the more constrained the Top-K operation the less accuracy achieved. Constraining Top-K results in selecting some activations or weights which are quite small. Similarly, some essential activations and weights are discarded just to satisfy the constraint.

A.6 Periodic Top-K

We have shown there is a little variation in the ‘K-th’ largest element during training, and it remains approximately constant as training proceed. Therefore, the Top-K does not need to be computed every iteration and can be periodically computed after some iterations. We define the number of iterations between computing the threshold for Top-K as the “Top-K period”. Since the periodic Top-K used the same threshold during the entire period, therefore, it is crucial to confirm that periodic Top-K implementation does not adversely affect the sparsity during training. We dumped the amount of sparsity obtained in weights and activation using periodic Top-K with period 100 iteration with target sparsity of 90%. Figure 10 shows the sparsity during training using periodic Top-K implementation is concentrated around our targeted sparsity, and the fluctuation decreases as training proceeds confirming our hypothesis that chosen Top-K parameter stabilizes i.e. the Top-K threshold converge to a fixed value during the latter epochs.

A.7 Sparsification of Output Gradients During Back-Propagation

SWAT is different from meProp as it uses sparse weight and activation during back-propagation, whereas meProp uses sparse output gradients. Our sensitivity analysis shows that convergence is extremely sensitive to the sparsification of output gradients. We compare the performance of the meProp and SWAT with deep networks and complex datasets. To compare SWAT’s approach to that of meProp, we use a variant of SWAT-U that only sparsifies the backward pass; we shall refer to this version of SWAT-U as SAW (Sparse Activation and Weight back-propagation). Figure 11 shows SAW and meProp convergence of ResNet18 with the ImageNet dataset. It compares the performance of meProp at 30% and 50% sparsity to SAW at 80% sparsity. As we can see, meProp converges to a good solution at sparsity of 30%. However, at 50% sparsity, meProp suffers from overfitting and fails to generalize (between epochs 5 to 30), and at the same time, it is unable to reach an accuracy level

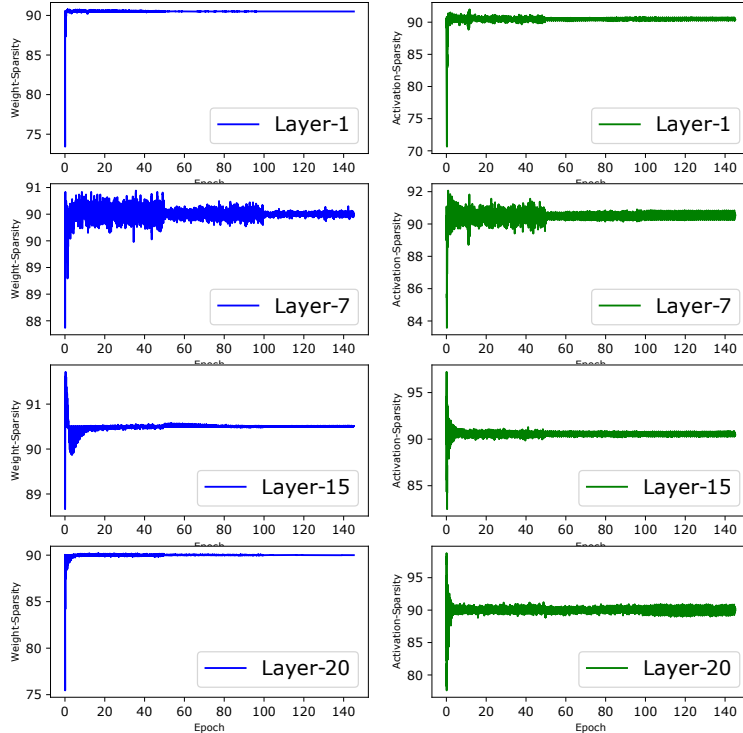


Figure 10: Sparsity Variation using Periodic Top-K Implementation. Network: ResNet-18, Dataset: CIFAR100, Top-K period: 100 iterations, Target Sparsity: 90%

above 45%. These results suggest that dropping output activation gradient (∇_{a_l}) is generally harmful during back-propagation. On the other hand, SAW succeeds to converge to a higher accuracy even at a sparsity of 80%.

Moreover, SWAT uses sparse weights and activations in the backward pass allowing compression of weights and activations in the forward pass. Effectively, reducing overall memory access overhead of fetching weights in the backward pass and activations storage overhead because only Top-K% activations are saved. This memory benefit is not present for meProp since dense weights and activations are needed in the backward pass, whereas there is no storage benefit of sparsifying the output gradients since they are temporary values generated during back-propagation.

A.8 Sparsification of Batch-Normalization Layer:

The activations and weights of BN layers are not sparsified in SWAT. Empirically, we found that sparsifying weights and activations are harmful to convergence. This is because the weight (gamma) of BN layers is a scaling factor for an entire output channel, therefore, making even a single BN weight (gamma) zero makes the entire output channel zero. Similarly, dropping activations affects the mean and variance computed by BN. Empirically we found that the BN layer is extremely sensitive to changes in the per channel mean and variance. For example, when ResNet18 is trained on CIFAR 100 using SWAT with 70% sparsity and we sparsify the BN layer activations, accuracy is degraded by 4.9% compared to training with SWAT without sparsifying the BN layers. Therefore, the activations of batch-normalization layer are not sparsified.

The parameters in a BN layer constitute less than 1.01% to the total parameters in the network and the total computation in the BN layer is less than 0.8% of the total computation in one forward and backward pass. Therefore, not sparsifying batch-normalization layers only affects the activation overhead in the backward pass.

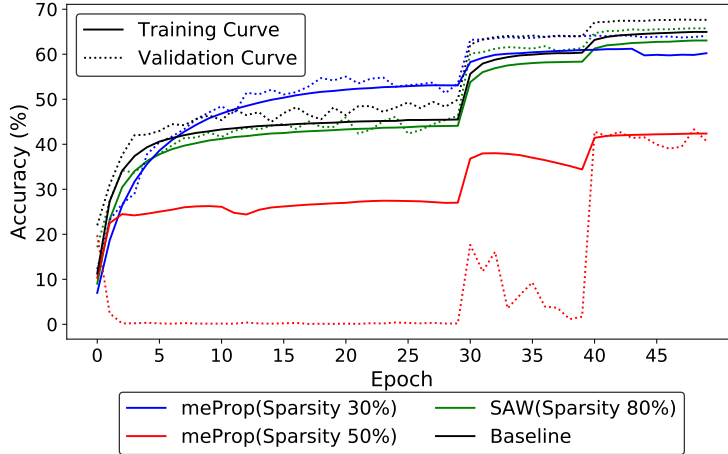


Figure 11: **Convergence Analysis:** Shows the training curve of ResNet18 on ImageNet for meProp and SAW algorithm. Learning rate is reduced by $\frac{1}{10}^{th}$ at 30^{th} and 40^{th} epoch.

A.9 Workstation Description

| WORKSTATION-DESCRIPTION | |
|-------------------------|--|
| CPU | Intel(R) Core(TM) i9-9900X CPU @ 3.50GHz Intel(R) Xeon(R) Silver 4116 CPU @ 2.10GHz |
| GPU | NVIDIA 2080-Ti |
| UBUNTU | Ubuntu 18.04.2 LTS |
| NVIDIA-DRIVER | 440.33.01 , 418.43 |
| CUDA, cuDNN | CUDA==10.0.130, cuDNN==7.501 |
| Pytorch | pytorch==1.1.0, torchvision==0.3.0 |

A.10 Details of implementation

We implemented all models and algorithms on pytorch framework. Code can be found at <https://github.com/AamirRaihan/SWAT>. To ease the reproducibility of our experiments, we have also created a docker image. We have also uploaded the model checkpoint on anonymous dropbox folder for easily verifying the trained model <https://www.dropbox.com/sh/vo4dxuogk40n6mg/AACdCWWhkhsYdqjjuvsvIb50a?dl=0>.

Table 11: Hyperparameters for ResNet, VGG and DenseNet experiments on CIFAR10/100

| Experiment | ResNet 18, 50, 101 | VGG 16 | DenseNet BC-121 |
|--|--|--|--|
| Number of training epochs | 150 | 150 | 150 |
| Mini-batch size (#GPU) | 128 (1) | 128 (1) | 64 (1) |
| Learning rate schedule (epoch range: learning rate) | 1 - 50: 0.100 51 - 100: 0.010 101- 150 : 0.001 | 1 - 50: 0.100 51 - 100: 0.010 101- 150 : 0.001 | 1 - 50: 0.100 51 - 100: 0.010 101- 150 : 0.001 |
| Optimizer | SGD with Momentum | SGD with Momentum | SGD with Momentum |
| Momentum | 0.9 | 0.9 | 0.9 |
| Nesterov Acceleration | False | False | False |
| Weight Decay | 5e-4 | 5e-4 | 5e-4 |
| TopK Implementation | TopK-NCHW | TopK-NCHW | TopK-NCHW |
| TopK Period | Per Iteration | Per Iteration | Per Iteration |

Table 12: Hyperparameters for WideResNet experiments on CIFAR10/100

| Experiment | WideResNet Depth=28 Widen Factor=10 |
|--|--|
| Number of training epochs | 200 |
| Mini-batch size (#GPU) | 128 (1) |
| Learning rate schedule (epoch range: learning rate) | 1 - 60: 0.100 61 - 120: 0.020 121- 160 : 0.004 161- 200 : 0.0008 |
| Optimizer | SGD with Momentum |
| Momentum | 0.9 |
| Nesterov Acceleration | True |
| Weight Decay | 5e-4 |
| Dropout Rate | 0.3 |
| TopK Implementation | TopK-NCHW |
| TopK Period | Per Iteration |
| Remarks | First and Last layer are not sparsified since the total parameters in these layers are less than 0.17% of the total network parameters |

Table 13: Hyperparameters for ResNet50/WRN-50-2 experiments on ImageNet

| Experiment | SWAT(UnStructured) | SWAT(Structured) |
|--|---|--|
| Number of training epochs | 90 | 90 |
| Mini-batch size (#GPU) | 256 (8) | 256 (8) |
| Learning rate schedule (epoch range: learning rate) | 1 - 30: 0.100 31 - 60: 0.010 61- 80 : 0.001 81- 90 : 0.0001 | 1 - 30: 0.100 31 - 60: 0.010 61- 80 : 0.001 81- 90 : 0.0001 |
| Learning Rate WarmUp | Linear (5 Epochs) | Linear (5 Epochs) |
| Optimizer | SGD with Momentum | SGD with Momentum |
| Momentum | 0.9 | 0.9 |
| Nesterov Acceleration | True | True |
| Weight Decay | 1e-4 | 1e-4 |
| Weight Decay on BN parameters | No | No |
| Label Smoothing | 0.1 | 0.1 |
| TopK Implementation | TopK-NCHW | TopK-Channel |
| TopK-Period | 1000 iteration | 1000 iteration |
| Remarks | First is not sparsified due to low parameters count. To speed up training, we used efficient Top-K implementation where the Top-K is computed periodically after 1000 iteration | |